Eur. Phys. J. B **59**, 29–34 (2007)
DOI: 10.1140/epjb/e2007-00273-5

The European
Physical Journal B

The electronic properties of SiCAlN quaternary compounds

Z.Q. Liu and J. Ni[a]

Department of Physics and Key Laboratory of Atomic and Molecular Nanoscience (Ministry of Education), Tsinghua University, Beijing 100084, P.R. China

Received 15 June 2007 / Received in final form 31 August 2007

Abstract. We have investigated the properties of SiCAlN quaternary compounds composed of SiC and AlN polytypes by first-principle calculations. We find that their band gaps have a large tunability and are sensitive to the polytype structures. Their electronic properties vary from wide-band-gap semiconducting to metallic due to the complex charge transfer between the two constituents SiC and AlN. The formation energies are also calculated. These results show SiCAlN quaternary compounds have potential applications in the electronic devices that can be tuned over a large wavelength range.

PACS. 74.70.Dd Ternary, quaternary, and multinary compounds – 71.20.Nr Semiconductor compounds – 71.20.-b Electron density of states and band structure of crystalline solids

1 Introduction

SiC and AlN are the wide-band-gap semiconductors which have been found many useful microelectronic and optoelectronic applications in the short-wavelength range of the visible spectrum and the near ultraviolet. SiC and AlN both exhibit polytypism. Of the more than 200 different polytypes of SiC [1], the most common ones are 3C-SiC (zinc-blende), 2H-SiC (wurtzite), 4H-SiC, 6H-SiC, and 15R-SiC. Depending on polytype, the low-temperature band gap of SiC ranges from 2.403 eV for 3C-SiC to 3.33 eV for 2H-SiC [2,3]. AlN usually has hexagonal wurtzite structure, but it has also been reported to be stabilized in the zinc-blende structure [4,5]. 4H-AlN and 6H-SiC polytypes have been grown via molecular-beam epitaxy (MBE) [6–9]. 2H-AlN has an experimental band gap of 6.28 eV [5,10], which is suitable as a gate dielectric material in potential SiC-based metal-insulator-semiconductor transistors [11]. The properties of SiC polytypes with indirect band gaps and AlN polytypes with very large band gaps have more or less limited their applications.

In recent years, multinary compounds have attracted much extensive research because of the larger tunability in their properties. Many experimental works have been attempted to grow SiCAlN quaternary compounds in view of the potential applications in electronic devices as well as coating materials. Early attempts of fabricating ceramic alloys in the SiC-AlN system use hot-pressing at very high temperatures in the range of 1700–2100 °C generally [12,13]. Later the $(\mathrm{SiC})_{1-x}(\mathrm{AlN})_x$ solid solution films are grown by MBE [14,15] and metal organic chemical vapour deposition [16,17] between 1000 °C and 1300 °C. Lately the growth of single-phase SiCAlN epitaxial films is accomplished by MBE at substrate temperatures of 500–750 °C [18–22]. The stoichiometric films grown by Roucka and Tolle et al. [20–22] have a predominantly wurtzite structure composed of 2H-SiC/2H-AlN and 4H-SiC/2H-AlN alternating layers along the hexagonal [0001] direction.

Previous calculations on SiCAlN compounds are mostly performed using $(\mathrm{SiC})_{1-x}(\mathrm{AlN})_x$ solid-solution models with the crystal structure of hexagonal wurtzite [20–22] or zinc-blende [23]. Recently, ordered structural models for $(\mathrm{SiC})_{1-x}$ $(\mathrm{AlN})_x$ ($x = 0.00$, 0.25, 0.50, 0.75, and 1.00) have been used by Tang et al. with wurtzite structure [24]. However, there are seldom calculated works on SiCAlN compounds composed of SiC and AlN polytypes. Because of the large difference between the band gaps of SiC and AlN polytypes, the band gaps of SiCAlN compounds composed of SiC and AlN polytypes are expected to have large tunability.

In this paper, we have studied the properties of SiCAlN structures composed of SiC and AlN polytypes by first-principle calculations. We find that their band gaps are sensitive to the polytype structures and compositions. Their electronic properties vary from wide-band-gap semiconducting to metallic due to the complex charge transfer between the two constituents SiC and AlN.

2 Structure models and computational details

Table 1 shows some of the simple SiC (or AlN) polytypes with four common notations [25,26]. All the SiC (or AlN)

---

[a] e-mail: `junni@mail.tsinghua.edu.cn`

Table 1. Some of the simple SiC (or AlN) polytypes with four common notations.

Ramsdell notation	Zhdanov notation	*hk* notation	*ABC* notation
2H	$\langle 1 \rangle$	*hh*	*AB*
3C	$\langle \infty \rangle$	*kkk*	*ABC*
4H	$\langle 2 \rangle$	*hkhk*	*ABCB*
6H	$\langle 3 \rangle$	*hkkhkk*	*ABCACB*
8H	$\langle 4 \rangle$	*khkkkhkk*	*ABACBABC*
15R	$\langle 23 \rangle$	*hkhkkhkhkkhkhkk*	*ABACBCACBABCBAC*

polytypes could be considered as the different arrangements of hexagonal or cubic Si-C (or Al-N) bilayers by stacking along the hexagonal [0001] or equivalent cubic [111] direction geometrically. 2H-SiC (or AlN) is the pure hexagonal stacking of Si-C (or Al-N) bilayers in the [0001] direction and 3C-SiC (or AlN) is the pure cubic stacking of Si-C (or Al-N) bilayers in the [111] direction. The other polytypes in the Ramsdell notation with nH-SiC (or AlN) (hexagonal) or nR-SiC (or AlN) (rhombohedral) can be considered as combinations of these two stacking sequences with the n Si-C (or Al-N) bilayers in the primitive cell. The 2H and 3C structures are the extremes in the parameter describing the percentage of hexagonal close packing (often called "hexagonality") with 100% and 0 respectively. The hexagonality is 50% for the 4H structure and about 33% for the 6H structure [27].

Suggested by the experimental findings [20–22], the SiCAlN structures in our study have the altering layers with the preferred interface bonding configurations of Si-N and Al-C. One SiC polytype and one AlN polytype stack together in each structure along the hexagonal [0001] or equivalent cubic [111] direction. We notate these structures with nH(C)mH(C) (n = 2, 3, 4, 6, 8, and m = 2, 3, 4, 6.), such as 3C2H and 2H2H denote 3C-SiC/2H-AlN and 2H-SiC/2H-AlN respectively. So the SiCAlN structures nH(C)mH(C) (n = 2, 3, 4, 6, 8, and m = 2, 3, 4, 6.) can be considered as the different arrangements of hexagonal or cubic Si-C and Al-N bilayers by stacking along the hexagonal [0001] or the equivalent cubic [111] direction geometrically. The primitive hexagonal unit cells of the 2H2H and 2H4H structures are shown in Figure 1. The hexagonal Cartesian coordinate system as well the primitive lattice vectors are given in the upper left corner of the figure. The initial lattice constants and atom coordinates are set with the linear average of those of SiC and AlN polytypes according to the Vegard's rule. All the structures are fully relaxed with cell volume and shape both allowed to change in our calculations.

The calculations have been performed using VASP (Vienna Ab initio Simulation Package) [28]. The approach is based on an iterative solution of the Kohn-Sham equations of the Density-Functional-Theory in a plane wave basis set with the Vanderbilt ultrasoft pseudopotentials [29]. We use the exchange-correlation functional with the generalized gradient approximation given by Perdew and Wang [30]. We set the plane wave cut-off energy to be 600 eV and the convergence of the force on each atom to be less than 0.01 eV/Å to optimize the lattice constants and the atom coordinates. The mesh of Gamma centered grids $16 \times 16 \times n$ is used to sample the Brillouin zone where n is adjusted between 3 and 8 according to the unit cell size in order to minimize systematic errors when the total energies of different structures are compared.

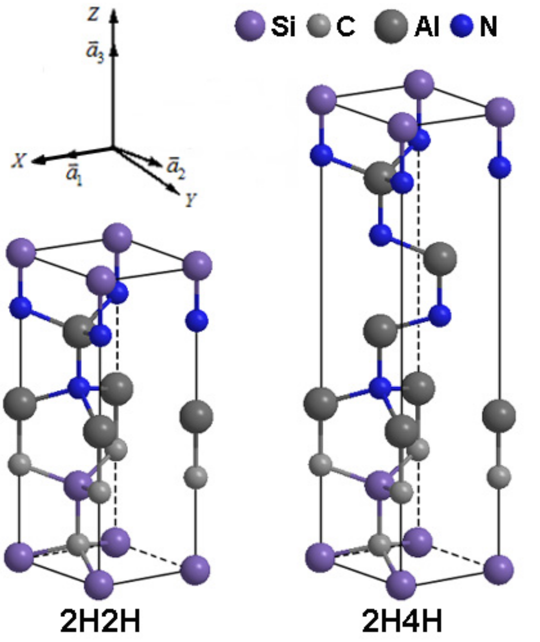

Fig. 1. (Color online) The primitive hexagonal unit cells of the 2H2H and 2H4H structures. The hexagonal Cartesian coordinate system as well the primitive lattice vectors are given in the upper left corner of the figure.

3 Results and discussion

The calculated lattice constants a and c of various SiCAlN compounds composed of SiC and AlN polytypes are shown in Table 2. We can see that the lattice constant a of nH(C)mH(C) (n = 2, 3, 4, 6, 8, and m = 2, 3, 4, 6.) decreases monotonically as n increases with m kept constant, for example, a(2H2H) > a(3C2H) > a(4H2H) > a(6H2H) > a(8H2H). The lattice constant a increases as the AlN constituent varies from 3C-AlN to 2H-AlN, 4H-AlN, and 6H-AlN, for example, a(2H3C) < a(2H2H) < a(2H4H) < a(2H6H).

Now, we analyze the band-gap variation tendency of SiCAlN compounds with change of polytype structures and compositions. Figure 2 shows the calculated band gaps of various SiCAlN structures. The x-coordinate

Table 2. The calculated lattice constants a and c in Å of various SiCAlN compounds composed of SiC and AlN polytypes. The first value in the table is lattice constant a and the second is c of the corresponding SiCAlN compound. The notation nH(C)- ($n = 0, 2, 3, 4, 6, 8.$) represents the SiC constituent. The notation -mH(C) ($m = 0, 2, 3, 4, 6.$) represents the AlN constituent. 0H- and -0H represent there are no SiC and AlN constituent in corresponding structures, respectively.

	$-0H$	−2H	−3C	−4H	−6H
0H−		3.1165,4.9956	3.1001, 7.5913	3.1067, 10.0697	3.1042, 15.1330
2H−	3.0851, 5.0634	3.0980, 10.0989	3.0940, 12.6702	3.0991, 15.1525	3.0996, 20.2056
3C−	3.0902, 7.5691	3.0950, 12.6405	3.0930, 15.2094	3.0965, 17.7061	3.0970, 22.7710
4H−	3.0873, 10.1076	3.0929, 15.1769	3.0916, 17.7406	3.0947, 20.2406	3.0956, 25.3022
6H−	3.0882, 15.1540	3.0913, 20.2405	3.0908, 22.7993	3.0931, 25.3079	3.0941, 30.3719
8H−	3.0886, 20.2001	3.0910, 25.2907	3.0907, 27.8522	3.0922, 30.3650	3.0930, 35.4324

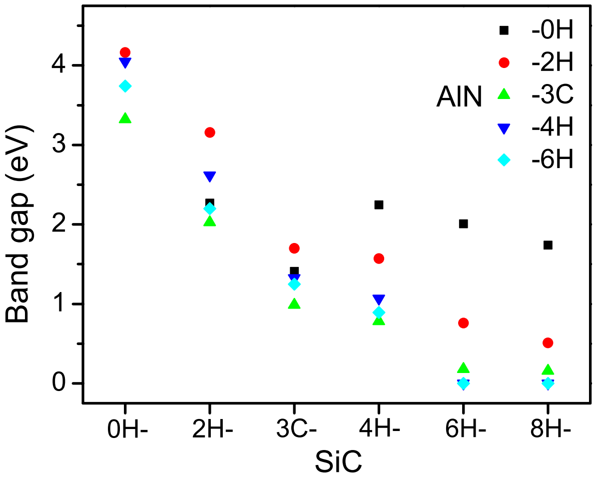

Fig. 2. (Color online) The band gaps of various SiCAlN structures.

nH(C)- ($n = 0, 2, 3, 4, 6, 8.$) represents that the SiC constituent in SiCAlN unit cells is 0H-SiC (no SiC constituent and structures are pure AlN polytypes), 2H-SiC, 3C-SiC, 4H-SiC, 6H-SiC, and 8H-SiC, respectively. The notation -mH(C) ($m = 0, 2, 3, 4, 6.$) represents that the AlN constituent in SiCAlN unit cells is 0H-AlN (no AlN constituent and structures are pure SiC polytypes), 2H-AlN, 3C-AlN, 4H-AlN, and 6H-AlN, respectively. We can see that the band gap of nH(C)mH(C) decreases monotonically as n increases with m kept constant, for example, E_g(2H-AlN) $>$ E_g(2H2H) $>$ E_g(3C2H) $>$ E_g(4H2H) $>$ E_g(6H2H) $>$ E_g(8H2H). The band gap of nH(C)mH(C) decreases as the hexagonality of AlN constituent decreases with n kept constant, for example, E_g(2H2H) $>$ E_g(2H4H) $>$ E_g(2H6H) $>$ E_g(2H3C). 6H4H, 6H6H, 8H4H and 8H6H marked with zero band gap values in Figure 2 are metallic. For 6HmH(C) and 8HmH(C), the electronic property varies from semiconducting to metallic as the AlN constituent changes from 2H-AlN to 6H-AlN. For nH(C)4H and nH(C)6H, the electronic property varies from semiconducting to metallic as the SiC constituent changes from 2H-SiC to 8H-SiC. Therefore, the electronic properties of SiCAlN compounds nH(C)mH(C) vary from wide-band-gap semiconducting to metallic. These results show that the SiCAlN quaternary compounds nH(C)mH(C) can be tailored by the polytype structures and compositions. This can have potential applications in the electronic devices that can be tuned over a large wavelength range.

The band gaps of SiC polytypes are 2.268 eV for 2H-SiC, 1.408 eV for 3C-SiC, 2.246 eV for 4H-SiC, and 2.006 eV for 6H-SiC respectively, in agreement with the results of other first-principle calculations [27,31,32]. They are about 1 eV lower than the experimental values [2,3] due to the underestimation of first-principle calculations. The band gaps of 2H-AlN and 3C-AlN are 4.163 eV and 3.323 eV respectively, in agreement with the results of other first-principle calculations [33–37]. The experimental value of the band gap of 2H-AlN is 6.28 eV [5,10]. There are seldom theoretical and experimental works on the electronic properties of 4H-AlN and 6H-AlN. We find that the band gaps of 4H-AlN and 6H-AlN are 4.05 eV and 3.742 eV respectively. In the experiments [20–22] for films with a kind of stacking of 2H2H and 4H2H structures, the band gap is about 3.2 eV. We predict that the band gaps of the films composed of 2H2H and 4H2H are in the range of 1.57–3.156 eV, which is consistent with the experimental results considering the underestimation of first-principle calculations.

The total densities of states (DOS) of nH(C)2H and 2HmH(C) are shown in Figure 3 and Figure 4, respectively. We can see that Fermi level (E_F) of nH(C)2H increases when the SiC constituent varies from 2H-SiC to 8H-SiC. E_F of 2HmH(C) has almost the same value. We can see that the valence band maximum (VBM) of nH(C)2H increases while the conduction band minimum (CBM) decreases with SiC constituent varying from 2H-SiC to 8H-SiC. For nH(C)3C, nH(C)4H, and nH(C)6H, the VBM also increases while the CBM decreases with SiC constituent varying from 2H-SiC to 8H-SiC. The VBM of 2HmH(C) keeps almost constant while the CBM decreases as the hexagonality of AlN constituent decreases. For 3CmH(C) and 4HmH(C), the VBM also keeps almost constant while the CBM decreases as the hexagonality of AlN constituent decreases.

We show the partial densities of states (PDOS) of 4H2H and 2H4H in Figures 5a and 5b, respectively. The PDOS from the contribution of p state of each atom in corresponding unit cell is plotted. In Figure 5, the atoms

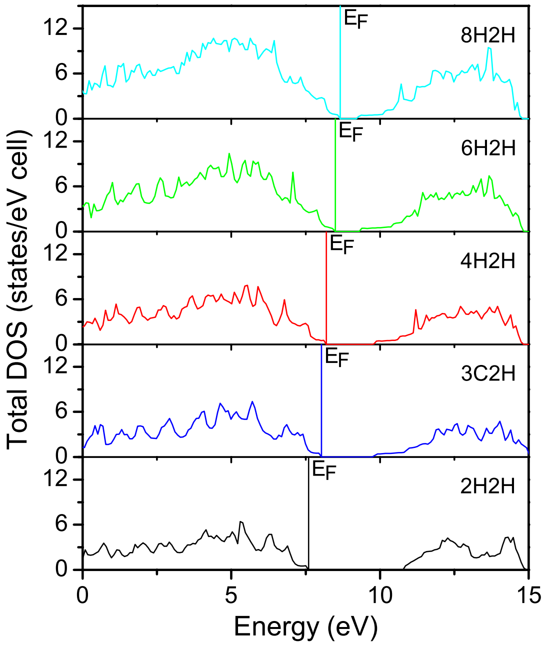

Fig. 3. (Color online) The total densities of states (DOS) of nH(C)2H.

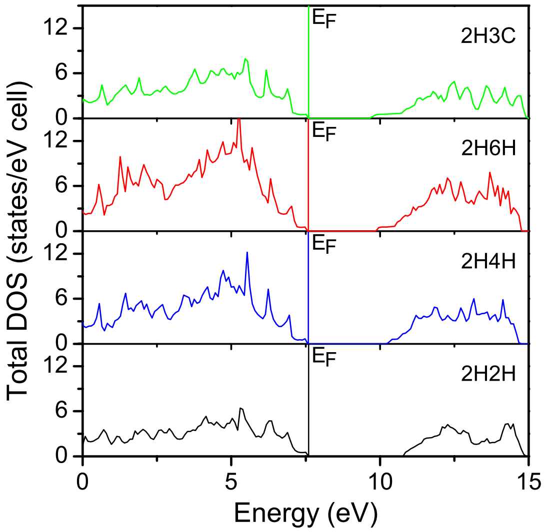

Fig. 4. (Color online) The total densities of states (DOS) of 2HmH(C).

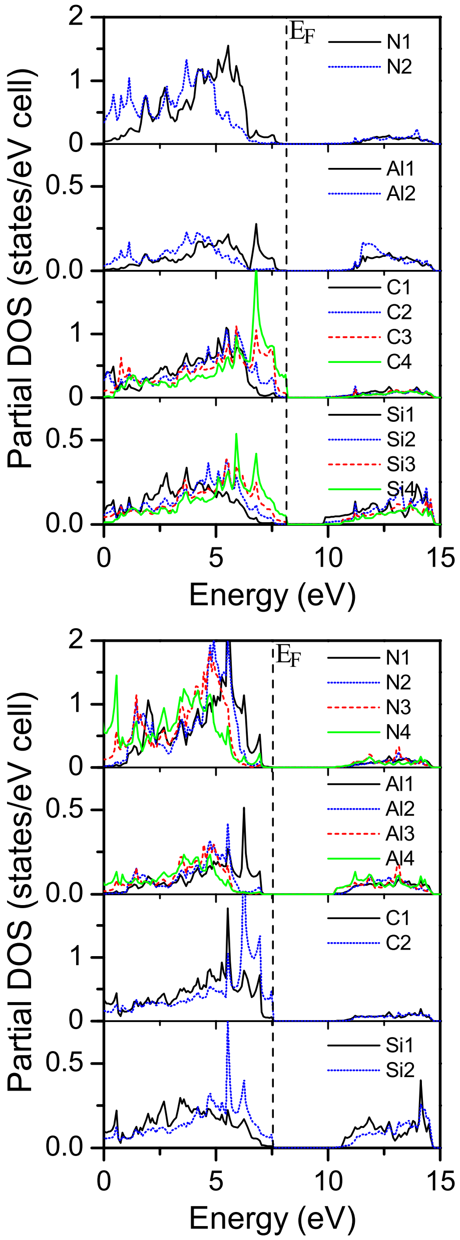

Fig. 5. (Color online) The partial densities of states (PDOS) of (a) 4H2H and (b) 2H4H. The PDOS from the contribution of p state of each atom in corresponding unit cell is plotted.

with the biggest or smallest serial number are close to the interface. From Figure 5, we can see that the VBM is mainly produced by the C atoms close to the C-Al interface. The CBM of 4H2H is mainly produced by the Si atoms close to the Si-N interface. The CBM of 2H4H is mainly produced by the Al atoms close to the Si-N interface. Therefore, the VBM of 4H2H and 2H4H origins from the SiC constituent. The CBM of 4H2H origins from the SiC constituent while that of 2H4H origins from the AlN constituent. By analyzing the PDOS of other SiCAlN compounds, we find that the VBM of nH(C)mH(C) origins from the SiC constituent. The CBM of nH(C)mH(C) origins from the SiC constituent when n is larger than m. The CBM of nH(C)mH(C) origins from the AlN constituent when n is smaller than m. Thus, we can understand why the VBM of 2HmH(C) almost keeps constant while the CBM decreases as the hexagonality of AlN constituent decreases. Since the SiC constituent of 2HmH(C) is always 2H-SiC, the VBM keeps constant. The CBM of 2HmH(C) is decided by AlN constituent. Therefore, the CBM of 2HmH(C) has the same variation as those of AlN polytypes, which decreases as the hexagonality decreases. We have $E_g(\text{2H2H}) > E_g(\text{2H4H}) > E_g(\text{2H6H}) > E_g(\text{2H3C})$. Thus, the band gap of nH(C)mH(C) decreases as the hexagonality of AlN constituent decreases with n kept constant.

Table 3. The formation energies $E_b[n\mathrm{H(C)}m\mathrm{H(C)}]$ of various SiCAlN compounds in eV.

E_b (eV)	−2H	−3C	−4H	−6H
2H−	0.23646	0.29175	0.28252	0.30570
3C−	0.27059	0.33659	0.34425	0.38229
4H−	0.30721	0.39116	0.41334	0.47013
6H−	0.34786	0.45462	0.50170	0.58557
8H−	0.37248	0.49596	0.55944	0.65939

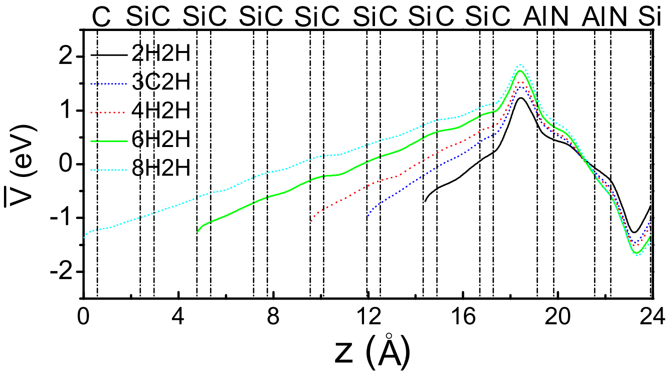

Fig. 6. (Color online) The averaged electrostatic potentials of nH(C)2H in one period along the hexagonal [0001] or equivalent cubic [111] direction.

The band-gap variation of SiCAlN compounds with change of the SiC constituent can be understood by analyzing the charge transfer between the two constituents SiC and AlN. In the binary semiconductors with a perfect tetrahedral lattice, there are four equivalent bonds for each atom. Each bond is occupied by two electrons. In the SiCAlN structures, C-Al and Si-N bonds are formed where the valence sum is different from eight and thus the bond occupation is different from two. Each C-Al bond is deficient by 1/4 of an electron, while each Si-N bond contains an excess of 1/4 of an electron. The excess charge can either occupy the antibonding orbital or be transferred to another partially occupied bond. Thus, we call the Si-N bonds donor bonds, since they donate part of an electron, and the C-Al bonds acceptor bonds [38]. Si-N donor bonds form donor interface and C-Al acceptor bonds form acceptor interface perpendicular to hexagonal [0001] or equivalent cubic [111] direction. The excess electrons around the Si-N donor interface could be transferred to the C-Al acceptor interface, which results in a positive and negative charge accumulation at the two interfaces respectively. Therefore a electric field occurs which is given by $E = \sigma_e/\varepsilon$ using the expression of electric field between the two capacitor plates charged with $\pm\sigma_e$ electrons per unit area [39]. Due to the electric field, a zigzag potential arises in the SiCAlN structures. We have calculated the averaged electrostatic potentials [40,41]. Figure 6 shows the averaged electrostatic potentials of nH(C)2H in one period along the hexagonal [0001] or equivalent cubic [111] direction. For nH(C)2H, the CBM and VBM are both controlled by the SiC constituent. The VBM and CBM are at the two opposite ends of SiC constituent in real space. Thus, the VBM of nH(C)2H increases while the CBM decreases with the increase of the thickness of SiC layers when the SiC constituent varies from 2H-SiC to 8H-SiC. We have $E_g(\mathrm{2H2H}) > E_g(\mathrm{3C2H}) > E_g(\mathrm{4H2H}) > E_g(\mathrm{6H2H}) > E_g(\mathrm{8H2H})$. So the band gap of nH(C)mH(C) decreases monotonically as n increases with m kept constant. A metallic state would result for thick SiC constituent as the CBM becomes lower than the VBM. As we can see that nH(C)4H and nH(C)6H vary from semiconducting to metallic as SiC constituent changes from 2H-SiC to 8H-SiC.

In the following, we discuss the stability of various SiCAlN structures. Using the total energies E_{tot} of SiCAlN quaternary compounds nH(C)mH(C) and those of the corresponding bulk SiC and AlN polytypes, the formation energies $E_b[n\mathrm{H(C)}m\mathrm{H(C)}]$ can be obtained as follows: $E_b[n\mathrm{H(C)}m\mathrm{H(C)}]= E_{tot}[n\mathrm{H(C)}m\mathrm{H(C)}]$-$E_{tot}[n\mathrm{H(C)}$-SiC]- $E_{tot}[m\mathrm{H(C)}$-AlN]. The results are shown in Table 3. We find that $E_b[n\mathrm{H(C)}m\mathrm{H(C)}]$ increases as the SiC constituent varies from 2H-SiC to 8H-SiC or the AlN constituent varies from 2H-AlN to 6H-AlN except that 2H3C is slightly higher in formation energy than 2H4H. Thus 2H2H has the lowest formation energy. This is in agreement with the experimental results [20–22] of the stoichiometric films with a predominantly wurtzite structure composed of 2H2H and 4H2H. All the formation energy values are positive which implies that the nH(C)mH(C) structures are metastable. The formation energies E_b of nH(C)mH(C) increase while their band gaps decrease as the SiC constituent varies from 2H-SiC to 8H-SiC. Thus lower band gaps would lead to higher formation energies.

4 Conclusions

In summary, we have performed the first-principle calculations to study the properties of SiCAlN quaternary compounds nH(C)mH(C). We find that 2H2H structure has the lowest formation energy which is in agreement with the experimental results. The band gap of nH(C)mH(C) decreases monotonically with the increase of the thickness of SiC layers when the SiC constituent varies from 2H-SiC to 8H-SiC. The band gap also decreases as the hexagonality of AlN constituent decreases. The electronic properties of nH(C)mH(C) vary from wide-band-gap semiconducting to metallic and can be tailored by the polytype structures and compositions. These results show that the SiCAlN quaternary compounds have potential applications in the electronic devices that can be tuned over a large wavelength range.

This research was supported by the National Natural Science Foundation of China (Grant No. 10674076) and the National Basic Research Program of China (Grant No. 2006CB605105).

References

1. N.W. Jepps, T.F. Page, Progr. Cryst. Growth Charact. **7**, 259 (1983)
2. P. Masri, Surf. Sci. Rep. **48**, 1 (2002)
3. O. Madelung, M. Schulz, H. Weiss, in *Semiconductors, Physics of Group IV Elements and III-V compounds*, edited by K.H. Hellwege, O. Madelung, Landolt-Börnstein, New Series, Group III, Vol. **17**, Pt. a (Springer-Verlag, Berlin, 1982)
4. V. Lebedev, V. Cimalla, U. Kaiser, Ch. Foerster, J. Pezoldt, J. Biskupek, O. Ambacher, J. Appl. Phys. **97**, 114306 (2005)
5. *Properties of Group-III Nitrides*, edited by J.H. Edgar, EMIS Datareviews Series (IEE, London, 1994)
6. N. Onojima, J. Suda, T Kimoto, H. Matsunami, Appl. Phys. Lett. **83**, 5208 (2003)
7. R. Armitage, J. Suda, T. Kimoto, Appl. Phys. Lett. **88**, 011908 (2006)
8. M. Horita, J. Suda, T. Kimoto, Appl. Phys. Lett. **89**, 112117 (2006)
9. D.M. Schaadt, O. Brandt, A. Trampert, H.-P. Schönherr, K.H. Ploog, J. Cryst. Growth **300**, 127 (2007)
10. P.B. Perry, R.F. Rutz, Appl. Phys. Lett. **33**, 319 (1978)
11. J. Choi, R. Puthenkovilakam, J.P. Chang, Appl. Phys. Lett. **86**, 192101 (2005)
12. R. Ruh, A. Zangvil, J. Am. Ceram. Soc. **65**, 260 (1982)
13. W. Rafaniello, M.R. Plichta, A.V. Virkar, J. Am. Ceram. Soc. **66**, 272 (1983)
14. R.S. Kern, L.B. Rowland, S. Tanaka, R.F. Davis, J. Mater. Res. **8**, 1477 (1993)
15. R.S. Kern, L.B. Rowland, S. Tanaka, R.F. Davis, J. Mater. Res. **13**, 1816 (1998)
16. I. Jenkins, K.G. Irvine, M.G. Spencer, V. Dmitriev, N. Chen, J. Cryst. Growth **128**, 375 (1993)
17. G.K. Safaraliev, Yu.M. Tairov, V.F. Tsvetkov, Sov. Phys. Semicond. **25**, 865 (1991)
18. R. Roucka, J. Tolle, D.J. Smith, P.A. Crozier, I.S.T. Tsong, J. Kouvetakis, Appl. Phys. Lett. **79**, 2880 (2001)
19. J. Tolle, R. Roucka, P.A. Crozier, A.V.G. Chizmeshya, I.S.T. Tsong, J. Kouvetakis, Appl. Phys. Lett. **81**, 2181 (2002)
20. R. Roucka, J. Tolle, A.V.G. Chizmeshya, P.A. Crozier, C.D. Poweleit, D.J. Smith, I.S.T. Tsong, J. Kouvetakis, Phys. Rev. Lett. **88**, 206102 (2002)
21. J. Tolle, R. Roucka, A.V.G. Chizmeshya, P.A. Crozier, D.J. Smith, I.S.T. Tsong, J. Kouvetakis, Solid State Sci. **4**, 1509 (2002)
22. R. Roucka, J. Tolle, A.V.G. Chizmeshya, P.A. Crozier, C.D. Poweleit, D.J. Smith, J. Kouvetakis, I.S.T. Tsong, Appl. Surf. Sci. **212-213**, 872 (2003)
23. A. Zaoui, M. Certier, M. Ferhat, O. Pagès, H. Aourag, Phys. Stat. Sol. (b) **205**, 587 (1998)
24. Y.-H. Tang, M.-H. Tsai, J. Appl. Phys. **97**, 103702 (2005)
25. A.R. Verma, P. Krishna, *Polymorphism and Polytypism in Crystals* (Wiley, New York, 1966)
26. S. Nakashima, H. Katahama, Y. Nakakura, A. Mitsuishi, Phys. Rev. B **33**, 5721 (1986)
27. C.H. Park, B.-H. Cheong, K.-H. Lee, K.J. Chang, Phys. Rev. B **49**, 4485 (1994)
28. G. Kresse, J. Hafner, Phys. Rev. B **47**, R558 (1993); Phys. Rev. B **49**, 14251 (1994); G. Kresse, J. Furthmüller, Comput. Mater. Sci. **6**, 15 (1996); Phys. Rev. B **54**, 11169 (1996)
29. D. Vanderbilt, Phys. Rev. B **41**, R7892 (1990)
30. J.P. Perdew, J.A. Chevary, S.H. Vosko, K.A. Jackson, M.R. Pederson, D.J. Singh, C. Fiolhais, Phys. Rev. B **46**, 6671 (1992)
31. C. Persson, U. Lindefelt, Phy. Rev. B **54**, 10257 (1996)
32. Z.Y. Jiang, X.H. Xu, H.S. Wu, F.Q. Zhang, Z.H. Jin, Solid State Commun. **123**, 263 (2002)
33. C. Perssona, A. Ferreira da Silvab, R. Ahujaa, B. Johansson, J. Cryst. Growth **231**, 397 (2001)
34. P. Jonnard, N. Capron, F. Semond, J. Massies, E. Martinez-Guerrero, H. Mariette, Eur. Phys. J. B **42**, 351 (2004)
35. R. Ahmed, H. Akbarzadehb, Fazal-e-Aleem, Physica B **370**, 52 (2005)
36. C. Stampfl, C.G. van de Walle, Phy. Rev. B **59**, 5521 (1999)
37. D. Vogel, P. Krüger, J. Pollmann, Phy. Rev. B **55**, 12836 (1997)
38. A. Kley, J. Neugebauer, Phys. Rev. B **50**, 8616 (1994)
39. R. Eppenga, Phys. Rev. B **40**, 10402 (1989)
40. A. Baldereschi, S. Baroni, R. Resta, Phys. Rev. Lett. **61**, 734 (1988)
41. S. Baroni, R. Resta, A. Baldereschi, M. Peressi, in *Spectroscopy of Semiconductor Microstructures*, edited by G. Fasol, A. Fasolino, P. Lugli, NATO Advanced Study Institutes Ser. (Plenum, New York, 1989), B Vol. **206**, p. 251